HHS Public Access

Author manuscript

Cell Rep. Author manuscript; available in PMC 2019 January 11.

Published in final edited form as:

Cell Rep. 2018 November 20; 25(8): 2110–2120.e3. doi:10.1016/j.celrep.2018.10.076.

The NF-κB Factor *Relish* Regulates Atg1 Expression and Controls Autophagy

Anubhab Nandy[1], **Lin Lin**[2], **Panagiotis D. Velentzas**[2], **Louisa P. Wu**[3], **Eric H. Baehrecke**[2], and **Neal Silverman**[1,4,*]

[1]Department of Medicine, University of Massachusetts Medical School, Worcester, MA 01605, USA

[2]Department of Molecular, Cell and Cancer Biology, University of Massachusetts Medical School, Worcester, MA 01605, USA

[3]Department of Cell Biology and Molecular Genetics, University of Maryland, College Park, MD 20742, USA

[4]Lead Contact

SUMMARY

Macroautophagy and cell death both contribute to innate immunity, but little is known about how these processes integrate. *Drosophila* larval salivary glands require autophagy for developmentally programmed cell death, and innate immune signaling factors increase in these dying cells. Here, we show that the nuclear factor κB (NF-κB) factor Relish, a component of the immune deficiency (Imd) pathway, is required for salivary gland degradation. Surprisingly, of the classic Imd pathway components, only Relish and the PGRP receptors were involved in salivary gland degradation. Significantly, *Relish* controls salivary gland degradation by regulating autophagy but not caspases. In addition, expression of either *Relish* or *PGRP-LC* causes premature autophagy induction and subsequent gland degradation. *Relish* controls autophagy by regulating the expression of *Atg1*, a core component and activator of the autophagy pathway. Together these findings demonstrate that a NF-κB pathway regulates autophagy during developmentally programmed cell death.

Graphical Abstract

*Correspondence: neal.silverman@umassmed.edu.

AUTHOR CONTRIBUTIONS

A.N., N.S, E.H.B., L.L., P.D.V., and L.W. designed experiments; A.N., L.L., and P.D.V. performed experiments; and A.N., N.S., and E.H.B. wrote the manuscript.

DECLARATION OF INTERESTS

The authors declare no competing interests.

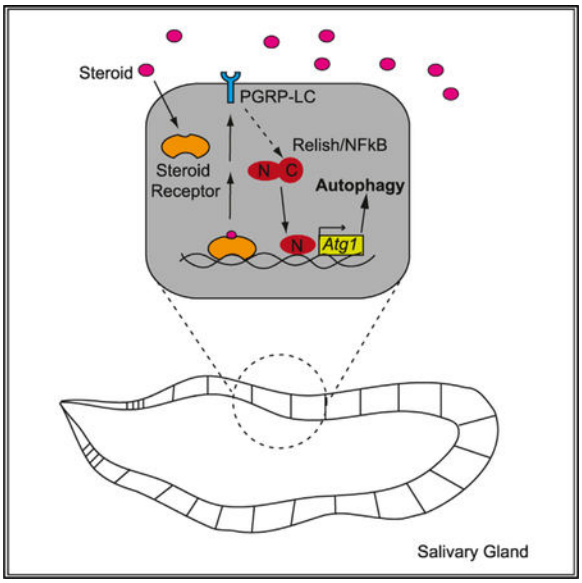

In Brief

Nandy et al. show that *Drosophila* peptidoglycan (*PGRP*) receptors and NF-kB factor *Relish* drive salivary gland degradation by controlling the expression of *Atg1*, a key component of the autophagy pathway.

INTRODUCTION

The nuclear factor κB (NF-κB) family of transcription factors is involved in a diverse range of physiological processes, including cell division, cell death, and most prominently innate and adaptive immunity (Bonizzi and Karin, 2004; Guttridge et al., 1999; Hayden and Ghosh, 2011). The mammalian NF-κB family consists of five members—RelA (p65), RelB, c-Rel, p50/p105, and p52/p100. These factors are critical for the production of cytokines, regulation of cell death, and control of cell cycle progression in activated leukocytes and lymphocytes. Mutation in these factors leads to lethality, increased susceptibility to infection, and altered tissue development, while constitutively active NF-κB leads to inflammatory diseases such as arthritis, inflammatory bowel disease, and cancer (Li and Verma, 2002). The study of NF-κB factors and their proper regulation remains of great interest for many fields.

One powerful model to study the role of NF-κB factors in diverse areas of biology is the fruit fly *Drosophila melanogaster,* which encodes three NF-κB factors—*Dorsal*, *Dif*, and *Relish*. *Dorsal* and *Dif* are similar to mammalian RelA and are activated following the cleavage of the cytokine Spätzle and its subsequent binding to and activation of the receptor Toll (Buchon et al., 2014). By contrast, *Relish* is an important component of the immune deficiency (Imd) pathway, which responds to diaminopimelic acid (DAP)-type peptidoglycan, from the cell wall of Gram-negative bacteria. Upon direct binding of DAP-type peptidoglycan to the peptidoglycan recognition protein-LC or peptidoglycan recognition protein-LE (PGRP-LC or PGRP-LE), a signaling cascade is triggered that

results in the cleavage, activation, and nuclear translocation of *Relish* and transcription of antimicrobial peptide (AMP) genes (Choe et al., 2002; Hedengren et al., 1999). AMPs such as Diptericin, Cecropin, and Defensin are small cationic peptides with direct antimicrobial activity (Imler and Bulet, 2005).

Relish was characterized as an important component of the *Drosophila* immune system and is primarily responsible for the immune-induced expression of AMP genes. However, recent findings implicate *Relish* in several cell death paradigms. For example, *Relish* is required for the death of photoreceptor cells in a *Drosophila* model of light-dependent retinal degeneration (Chinchore et al., 2012). In another report, *Relish* was found to play a crucial role in elimination of ‘‘unfit’’ cells in a model of cell competition (Meyer et al., 2014). These findings suggest the involvement of *Relish* in caspase-dependent cell death pathways. Other reports have argued that Relish, through the production of AMPs, can drive other types of cell death and neurodegeneration in the *Drosophila* CNS (Cao et al., 2013; Petersen et al., 2013). Moreover, dying *Drosophila* larval salivary glands also show a marked increase in the expression of several NF-κB-dependent AMP genes (Lee et al., 2003). The salivary gland is an excellent genetic model to study developmentally programmed cell death as steroid-induced degradation of this tissue requires both apoptotic caspases and autophagy (Berry and Baehrecke, 2007)

Autophagy is a catabolic process that sequesters cytoplasmic components inside a double membrane ‘‘autophagosome’’ structure followed by lysosomal fusion and content degradation. Although different types of autophagy have been characterized (Mizushima and Komatsu, 2011), here we will use the word ‘‘autophagy’’ to denote macro-autophagy. Autophagy serves different roles depending on cellular and environmental context (He and Klionsky, 2009). In times of starvation, autophagy promotes cell survival by recycling cellular contents. Dysregulation of autophagy has been implicated in different age-related disorders, including neurodegeneration (Qin et al., 2003; Yu et al., 2004). Also, loss of autophagy contributes to genomic instability, tissue damage, and in turn cancer (Karantza-Wadsworth et al., 2007; Mathew et al., 2007; White, 2015). Moreover, autophagy is involved in several immune pathways including inflammatory signaling, immune mediator secretion, antigen presentation, and the elimination of cytosolic pathogens (Pengo et al., 2013; Saitoh et al., 2008; Schmid et al., 2007; Yano et al., 2008).

In *Drosophila*, autophagy and immune responses have been linked by several findings. The intracellular pathogen *L. monocytogenes* is controlled through the activation of autophagy following immune recognition by the cytosolic peptidoglycan receptor PGRP-LE (Yano et al., 2008). More recently, we found that complement-like factor Mcr also induces autophagy, via signaling through the scavenger receptor Draper, specifically in the salivary glands (Lin et al., 2017). Interestingly, we also observed that several AMP genes and other immune factors, which are controlled by NF-κB factors in the context of immunity, are upregulated in dying salivary glands (Lee et al., 2003). Together these findings suggested possible involvement of *Relish* and the Imd pathway in the control of autophagic cell death during salivary gland degradation.

Here we show that the *Drosophila* NF-κB family member *Relish* plays an essential role in salivary gland degradation. Surprisingly, apart from *Relish* and the two PGRP receptors involved in the Imd pathway, none of the other six components of the canonical Imd signaling pathway (*FADD*, *Dredd*, *IMD*, *Diap2*, *Tak1*, *IKKβ*, *IKKγ*) play any role in salivary gland cell death and degradation. The contribution of *Relish* to salivary gland degradation is caspase independent, unlike that observed in either the *Relish*-dependent cell competition or retinal degeneration models. On the other hand, *Relish* was necessary and sufficient for activation of autophagy in the salivary gland. Our genetic and molecular data further indicate that Relish regulates autophagy by controlling the expression of *Atg1*, a key activator of autophagy. This study reveals a role for known immune pathway components, the NF-κB factor *Relish* and PGRP receptors, in the regulation of autophagy during programmed cell death.

RESULTS

Relish Is Required for Salivary Gland Cell Death

Genome-wide transcriptome analyses of dying *Drosophila* salivary gland cells identified many genes that are either upregulated or downregulated during cell death (Lee et al., 2003). In addition to genes associated with apoptosis and autophagy, many NF-kB targets, including AMP genes, were upregulated in dying salivary glands. This prompted us to analyze whether loss of immunity genes would cause any change in salivary gland cell death.

We found that loss of the NF-kB factor *Relish* impaired salivary gland degradation. Salivary gland cell death is activated by a rise in steroid hormone 12 hr after puparium formation, and by 16 hr after puparium formation this tissue is largely degraded. Like wild-type animals, control animals (Rel^{E23}, an exact excision of the same P element used to create the Rel^{E20} allele; Hedengren et al., 1999) possessed no remnants of salivary glands 24 hr after puparium formation (APF) (Figures 1A and 1B). By contrast, a null allele of *Relish* (Rel^{E20}) exhibited persistent salivary gland cell fragments at 24 hr APF in 80% of the cases examined (Figures 1A, 1B, and 1A‘, displaying the salivary gland cell fragments without other tissue). The 24 hr APF time point was chosen as by this time salivary glands are completely degraded in wild-type animals and no salivary gland fragments are expected to persist.

In addition, ectopic expression of *Relish* in the salivary glands, using the GAL4 UAS system, rescued the salivary gland degradation defect observed in *Relish* mutant animals (Figures 1C and 1D). Together these results indicate that *Relish* is required for complete salivary gland degradation and clearance.

Relish is an essential component of *Drosophila* Imd pathway. Therefore, we next sought to determine if other components of the Imd pathway are also involved in salivary gland degradation. Surprisingly, only either *Relish* or *PGRP-LC* mutants or *PGRP-LC*, *PGRP-LE* double mutants displayed a significant defect in salivary gland degradation; none of the other Imd pathway components affected salivary gland destruction and clearance (Figures 1E, 1F, S1A–S1H, S2A, and S2B). We next tested whether other NF-kB factors function in salivary gland degradation. Neither *Dif* nor *Dorsal* mutants displayed any impairment in

salivary gland degradation when mutated either alone or together, further illustrating the specificity of *Relish* in salivary gland degradation (Figures S2C–S2H).

Major transcriptional targets of Relish during the immune response include the AMP genes. Previous transcriptomic analyses of the dying salivary glands showed upregulation of several AMP genes, including *Diptericin-A*, *Cecropin-C*, and *Attacin-A*. We analyzed RNA levels of these three AMPs at 0 to 14 hr APF in four mutant strains, but the expression pattern of these AMP genes did not show any association with the impact of mutants on salivary gland degradation, suggesting AMPs are not involved in this process (Figures S3A–S3C). Previous reports demonstrated that ectopic expression of AMPs could drive neurodegeneration (Cao et al., 2013). However, ectopic expression of several AMPs in the salivary gland did not result in any discernible effect (Figure S3D). In addition, ectopic expression of AMPs in salivary glands of *Relish* mutants failed to suppress the *Relish* gland degradation defects (Figures S3E–S3H), further indicating that AMPs do not function in salivary gland degradation. Together these data indicate AMP expression is not involved in salivary gland degradation.

We next considered the possibility that the endogenous microflora could provide a stimulus through the PGRPs, which are activated by the bacterial cell wall (Kaneko et al., 2004; Leulier et al., 2003), to activate *Relish* and contribute to salivary gland degradation. However, axenic flies, which were negative for bacterial 16S sequences and devoid of any colony forming microbes (Figures S4A and S4B), showed normal salivary gland degradation (Figures S4C and S4D), excluding a role for the microflora in salivary gland degradation. Combined, these data suggest that PGRP receptors and Relish function in a pathway to regulate cell death.

Relish Contributes to Autophagic, but Not Caspase-Dependent, Cell Death

Caspases and autophagy are both necessary for complete salivary gland degradation (Berry and Baehrecke, 2007). To determine if *Relish* contributes to the caspase-dependent pathway, p35, a potent baculoviral inhibitor of effector caspases, was expressed in the salivary glands of wild-type or Rel^{E20} mutant animals. As expected, p35 expression in the salivary glands of wild-type animals resulted in the accumulation of cell fragments in 60% of animals analyzed, with more intact tissue, known as gland fragments, in the other 40%. These gland fragments are indicative of a more severe failure in salivary gland degradation. When p35 was expressed in the *Relish* mutants, gland fragments were observed in 80% of animals (Figures 2A, 2B, and 2A‘, displaying the salivary gland fragments without other tissue). The enhanced severity of this phenotype suggests that *Relish*-mediated cell death and caspase-dependent apoptotic pathways are distinct, working in tandem contributing to salivary gland degradation.

Cleaved caspase-3 is used as a marker of caspase activity (Fan and Bergmann, 2010). The accumulation of cleaved caspase-3 in salivary glands was examined by immunofluorescence, and *Relish* had no effect on the appearance of this apoptotic marker (Figures 2C and 2D). Together, these results indicate that caspase-dependent and *Relish*-mediated cell death pathways function in parallel, converging on the degradation and clearance of the larval salivary gland.

We next examined the relationship between *Relish* and autophagy. Decreased *Atg18* function results in persistence of salivary gland cell fragments (Berry and Baehrecke, 2007), a phenotype that is similar to *Relish* mutants. In *Atg18*, *Relish* double mutants, salivary gland cell fragments were present 24 hr APF, similar to that observed in either single mutant (Figures 3A and 3B), suggesting *Relish* and autophagy regulate salivary gland degradation through a common pathway. To further examine the connection between *Relish* and autophagy, mCherry-Atg8a puncta were visualized in the dying gland 14 hr APF. Control animals showed distinct puncta in salivary gland cells, while the amount of Atg8a puncta were significantly decreased in the salivary glands of *Relish* mutant animals (Figures 3C and 3D). However, *Relish* does not appear to be required for all autophagic cell death pathways, as *Relish* mutants displayed normal midgut autophagic cell death (Figures S4E and S4F).

In *Drosophila*, the expression of *Atg1* induces premature autophagy in multiple *Drosophila* tissues (Berry and Baehrecke, 2007; Chang et al., 2013; Scott et al., 2007). We expressed *Atg1* in salivary glands to test if this is sufficient to suppress the *Relish* phenotype. Indeed, *Atg1* expression in the salivary glands of *Relish* mutants suppressed the salivary gland degradation defect observed in *Relish* mutants (Figures 3E and 3F). Taken together, these data indicate *Relish* is required for autophagy during salivary gland degradation.

Expression of Relish N Terminus or PGRP-LC Causes Premature Gland Degradation

Relish and *PGRP-LC* are crucial components of the Imd pathway, and expression of these factors can activate Imd signaling even without an immune challenge (DiAngelo et al., 2009; Gottar et al., 2002; Wiklund et al., 2009). Our data also suggest that *Relish* and *PGRP-LC* positively regulate salivary gland autophagic cell death pathway. Therefore, we hypothesized that expression of active versions of these factors would cause early gland degradation. To test this hypothesis, we expressed either full-length *Relish*, the N terminus of *Relish* (*RelN*, an active form), *PGRP-LCx*, *PGRP-LE*, *Dredd*, or *imd* in salivary glands and histologically analyzed 6 hr APF, long before salivary glands normally degrade. Salivary gland expression of either *RelN*, *PGRP-LC*, or *PGRP-LE* caused premature gland degradation, but no such phenotype was observed with similar expression of full-length *Relish*, *imd*, or *Dredd* (Figures 4A–4L; Figures S5A–S5D). Note the histological sections exhibited here were selected to include the maximum gland area, which is a more ventral slice than those displayed in the analysis at 24 hr, shown in earlier figures with loss-of-function phenotypes, and does not include as much brain tissue. Gland-specific expression of *RelN* or *PGRP-LC* caused a marked loss of lumen structure and a severe reduction of gland size. Similarly, expression of these genes in third-instar salivary glands also caused severe gland size reduction (Figures S5E–S5I). *Imd* expression caused a mild degree of gland size reduction in the third instar, while *Relish* full-length and *Dredd* had no effect. These data demonstrate that expression of active *Relish*, *PGRP-LCx*, or *PGRP-LE* in salivary glands is sufficient to trigger a pathway of gland degradation.

Premature Gland Degradation due to Relish and PGRP Expression Is Autophagy Dependent

We next tested if the early salivary gland degradation induced by *RelN* expression was dependent either on caspases or autophagy. *RelN* was expressed in salivary glands either

along with *p35* or in a homozygous *Atg18* mutant background. Inhibition of caspases by expression of *p35* did not suppress the early gland degradation caused by *RelN* expression (Figures 5A and 5B). By contrast, when *RelishN* was expressed in *Atg18* mutant animals, a complete suppression of early gland degradation was observed (Figures 5C and 5D).

Drosophila midgut cells undergo dramatic size reduction due to autophagy induction during pupation (Chang et al., 2013). Similarly, expression of either *RelN* or *PGRP-LCx* in salivary gland cell clones also caused significant cell-autonomous reduction and autophagy, as assayed by mCherry-Atg8a puncta formation in the expressing single-cell clones but not neighboring cells (Figures 5E–5H). Additionally, when expressed throughout the third-instar salivary gland, either *RelN* or *PGRP-LC* triggered Atg8a puncta formation. By contrast, expression of *imd* triggered only mild Atg8a puncta formation, while either *Relish* full-length or *Dredd* expression did not cause any Atg8a puncta formation (Figure S6A–S6E). Taken together, these data indicate that premature gland degradation caused by *RelN* and *PGRP-LC* misexpression is due to premature activation of autophagy.

Relish and PGRP-LCx Function Upstream of the Autophagy Pathway

To begin to map the pathway by which *Relish* and *PGRP-LC* control autophagy in salivary glands, we next determined the epistatic relationship between these two classic immune signaling components. *PGRP-LCx*-induced premature gland degradation was suppressed in *Relish* mutants (Figures 6A and 6B). However, *RelN*-induced early gland degradation was unaffected in LCx mutants (Figures 6C and 6D), indicating that *PGRP-LCx* acts upstream of *Relish*, as observed in the immune signaling context.

Earlier data indicate that *Relish* affects the autophagy pathway upstream of both *Atg8* and *Atg18* (Figures 3 and 5). To further map the interaction between *Relish* and the autophagy pathway, *RelN* misexpression was combined with either knockdowns or mutations of two genes upstream in the autophagy pathway, *Atg1* or *Atg13* (Figures 6E–6H). In particular, *RelN*-induced salivary gland degradation was suppressed by loss of *Atg1* but not by *Atg13*. These results suggest Relish acts upstream of *Atg1* but downstream of *Atg13*. Consistent with this model, *Atg1* overexpression was sufficient to drive salivary gland degradation in the absence *Atg13* (Figures S6F and S6G). Since *Relish* is best characterized as a transcriptional activator, we investigated whether *Relish* influences *Atg1* expression. The level of *Atg1* mRNA in the salivary glands of both control (Rel^{E23}) and *Relish* mutant animals (Rel^{E20}) was determined at both 0 hr and 14 hr APF. We found that expression of *Atg1* gene is significantly reduced at both time points in *Relish* mutants compared to controls (Figure 6I). However, the expression of multiple other autophagy genes was unaffected (Figure S6H–S6K). On the other hand, *RelN* expression in salivary glands significantly increased *Atg1* transcription (Figure 6J), and elevated *Atg1* expression is known to be sufficient to drive autophagy in the salivary gland (Berry and Baehrecke, 2007).

Our results suggest Relish may directly regulate *Atg1* expression. In fact, four potential kB sites were observed in the sequences upstream of the *Atg1* locus (Figure 6K). To determine if Relish binds to any of these putative kB sites and directly regulates *Atg1* expression, we performed a chromatin immunoprecipitation assay to detect RelN binding to the *Atg1* locus. Two of the kB sites (723, 26, closest to the transcript start site) displayed significant

enrichment for RelN binding (Figures 6K and 6L). Together these data argue that *Relish* controls autophagy through the direct regulation *Atg1* expression.

DISCUSSION

Different aspects of autophagy have been extensively studied, particularly during nutrient deprivation, and the role of metabolites in the regulation of autophagy is well established. Autophagy is critical for genomic stability and alleviation of oxidative stress and in turn the prevention of tumorigenesis (White, 2015). In recent years autophagy has become an attractive target for cancer therapy (Thorburn et al., 2014). Moreover, it has also been observed that autophagy plays important roles in different immune defenses, especially against intracellular pathogens.

Our findings suggest that the NF-κB factor *Relish*, an important component of the fly immune system, plays a significant role in steroid-hormone-triggered autophagy in the salivary glands of *Drosophila*. *Relish* positively regulates autophagy as evidenced by the inhibition of autophagy in salivary glands of *Relish* mutant flies. Ectopic expression of active *Relish* induces autophagy and causes premature gland degradation. Furthermore, we present a mechanism by which *Relish* regulates autophagy. *Relish* drives the expression of *Atg1*, which is both necessary and sufficient for autophagy induction and programmed cell death of salivary glands (Berry and Baehrecke, 2007; Scott et al., 2007).

As *Relish* is the key transcription factor regulating *Drosophila* immunity via the Imd pathway, we examined all other components of this pathway to determine whether they also contribute to salivary gland degradation. Surprisingly, apart from the bacterial sensing receptors—*PGRP-LC*, *PGRP-LE*—and *Relish,* no other Imd pathway components affected salivary gland degradation. *PGRP-LC* functions upstream of *Relish* during gland degradation, similar to that observed in the immune signaling context. These results are surprising and suggest two possibilities, either a direct interaction between Relish and PGRP-LC/ LE or the existence of a pathway that connects PGRP-LC and PGRP-LE to Relish without the involvement of other canonical Imd pathway components.

It has been reported that Imd pathway components can trigger cell death and/or autophagy in different contexts involving *PGRP* receptors and/or *Relish*, but the mechanism involved likely differ. For example, *Relish*, *Dredd*, and *Fadd* were found to be essential for the light-dependent death of photoreceptor cells in *norpA* mutant flies (Chinchore et al., 2012), while another report suggests that *Relish*, *Dredd*, and several *Drosophila Toll-Related Receptors* are crucial in removing less-fit cells in a *Drosophila* wing-disc model of apoptotic cell competition (Meyer et al., 2014). *Relish* has also been linked to neurodegeneration in *Drosophila*, where *Relish*-dependent expression of AMPs was shown to cause increased neuronal damage (Cao et al., 2013). Several of these studies either speculated or showed that *Relish* influences caspase-dependent cell death. It has also been reported that *PGRP-LE*, but not *Relish*, is crucial to mount an autophagic response against cytosolic *Listeria monocytogenes* infection (Yano et al., 2008). So clearly Imd pathway components can act either independently or together to cause cell death and/or autophagy, in different cellular

contexts. However, in salivary gland degradation, *Relish* does not affect caspase-dependent processes and instead controls the activation of autophagic cell death.

Previous research indicates that some autophagy components play important roles in both immunity and tumorigenesis, such as *ATG6/BECN1*, which acts downstream of cGAS-STING as well as TLR4 upon cytosolic DNA and lipopolysaccharide (LPS) exposure, respectively (Cadwell, 2016). Additionally, deletion of *BECN1* results in the generation of liver and lung tumors as well as lymphomas in mice (Qu et al., 2003). These results demonstrate that some autophagy components play dual roles in both immunity and cellular homeostasis, depending on the cellular context. Interestingly, our findings also demonstrate a dual role of the PGRP receptors and Relish in both immune responses and regulation of developmentally controlled cell death.

Our results clearly demonstrated that *PGRP-LC* and *PGRP-LE*, which encode receptors known to directly bind bacterial peptidoglycan, and the NF-κB transcription factor *Relish* function in salivary gland degradation. However, salivary gland degradation occurred normally in axenic flies, demonstrating that microbial triggers are not involved in this process. The lack of any microbial involvement suggests that the PGRPs and/or Relish are activated by developmental cues during salivary gland degradation. We have previously demonstrated that a rise in steroid hormone induces *PGRP-LC* and *Relish* expression (Rus et al., 2013). In fact, we also observed increased expression of both *PGRP-LC* and *Relish* in dying salivary glands (Figures S6L and S6M), and elevated levels of *PGRP-LC* are sufficient to activate the classical Imd pathway (Choe et al., 2002). Together these findings suggest a hypothesis whereby high levels of steroid upregulate *PGRP-LC* within the salivary glands to a level that triggers a non-classical *PGRP-LC/Relish* pathway, which in turn induces *Atg1* expression. *Atg1* expression per se is sufficient to activate autophagy in the salivary gland (Berry and Baehrecke, 2007), even in absence of *Atg13*. Hence, even in the absence of any microbial stimulus, steroid hormone signaling, through elevated expression of *PGRP-LC* and *Relish*, could contribute to the activation of programmed cell death by transcriptionally inducing *Atg1* and activating autophagy. Alternatively, in this context PGRPs could be activated by a yet-to-be identified developmentally regulated ligand to activate Relish and autophagy. Future studies will be necessary to discriminate between these possibilities.

STAR★METHODS

KEY RESOURCES TABLE

REAGENT or RESOURCE	SOURCE	IDENTIFIER
Antibodies		
Mouse anti-FLAG	Sigma Aldrich	Cat#F-1804; RRID: AB_262044
Rabbit anti-cleaved caspase 3	Cell Signaling Technology	Cat#9664; RRID: AB_2070042
Goat anti-rabbit alexa fluor 633	ThermoFisher	Cat#A-21070; RRID: AB_2535731
Chemicals, Peptides, and Recombinant Proteins		
PBS	GIBCO	70011
25% Glutaraldehyde	Electron Microscopy Sciences	16220

REAGENT or RESOURCE	SOURCE	IDENTIFIER
Paraformaldehyde	Electron Microscopy Sciences	15710
Triton X-100	Sigma Aldrich	T8787
Tween 20	Fisher	BP337–500
Vectashield	Vector Laboratories	H-1200
Tris-HCI	Sigma	T3253
NaCI	Fisher	BP358–212
BSA	Fisher	BP1600–100
16% Formaldehyde	ThermoFisher	28906
Glycine	Fisher BioReagents	BP-381–5
Proteinase-K	ThermoFisher	25530049
iScript gDNA clear DNA synthesis kit	Bio-Rad	1725035
SYBR Green	Bio-Rad	1725122
Grape Juice Agar	Genesee Scientific	47–102
EDTA	Quality Biological	351–027-101
Experimental Models: Organisms/Strains		
D. melanogaster, Canton-S	Bloomington Drosophila Stock Center	64349
D. melanogaster, Rel^{E20}	Fledengren et al., 1999	N/A
D. melanogaster, PGRP-LC$^{\Delta E}$	Gottar et al., 2002	N/A
D. melanogaster, PGRP-LE^{112};; PGRP-LC$^{\Delta E}$	Takehana et al., 2004	N/A
D. melanogaster, UAS-*p35*	Hay et al., 1994	N/A
D. melanogaster, Atg13^{D74}	Chang and Neufeld, 2009	N/A
D. melanogaster, UAS-*Atg1^{6A}*	Mohseni et al., 2009	N/A
D. melanogaster, Dredd^{D55}	Leulier et al., 2000	N/
D. melanogaster, Tak1^{2}	Vidal et al., 2001	N/A
D. melanogaster, UAS-AMPs	Cao et al., 2013	N/A
D. melanogaster, UAS-PGRP-LCx	Kaneko et al., 2006	N/A
D. melanogaster, UAS-Atg1 RNAi	Vienna Drosophila Research Center	16133
D. melanogaster, Df (J4)	Meng et al., 1999	N/A
D. melanogaster, Atg18a^{KG03090}	Bloomington Drosophila Stock Center	13945
D. melanogaster, Df(3L)Exel6112	Bloomington Drosophila Stock Center	7591
D. melanogaster, w; pmCherry-Atg8a	Denton et al., 2012	N/A
D. melanogaster, imd^{10191}	Pham et al., 2007	N/A
D. melanogaster, imd^{1}	Georgel et al., 2001	N/A
D. melanogaster, Diap2^{7C}	Leulier et al., 2006	N/A
Oligonucleotides		
Table S1	This study	N/A
Software and Algorithms		
ImageJ	NIH	https://imagej.nih.gov/ij/

REAGENT or RESOURCE	SOURCE	IDENTIFIER
AxioVision	Zeiss	N/A
Prism	Graphpad Software, Inc.	https://www.graphpad.com/cientific-software/prism/

CONTACT FOR REAGENT AND RESOURCE SHARING

Further information and requests for resources and reagents should be directed to and will be fulfilled by the Lead Contact, Neal Silverman (Neal.Silverman@umassmed.edu).

EXPERIMENTAL MODEL AND SUBJECT DETAILS

Fly Strains: All strains have been previously described including *Relish*^{E23}, a precise P-element excision allele, and *Relish*^{E20}, a congenic imprecise deletion allele (Hedengren et al., 1999), *PGRP-LCx*$^{\Delta E}$ and the *PGRP-LE*^{112};; *PGRP-LCx*$^{\Delta E}$ double mutant (Gottar et al., 2002; Takehana et al., 2004), *Diap2*^{7C} (Leulier et al., 2006), *Dredd*^{D55} (Leulier et al., 2000), *imd*^{10191} (Pham et al., 2007), *imd*^{1} (Georgel et al., 2001), UAS-*Relish Full length* (BL-9459) (Hedengren et al., 1999), UAS-*RelN* (Wiklund et al., 2009), UAS-*imd* (Georgel et al., 2001), UAS-*Dredd* (Leulier et al., 2002), *Tak1*^{2} (Vidal et al., 2001), UAS-*AMP*s (Cao et al., 2013), UAS-*PGRP-LCx* (Kaneko et al., 2006), hsflp; +, act < FRT, cd2, FRT > Gal4, *UAS-GFP*, *pmcherry-Atg8a* (Denton et al., 2012), UAS-*Atg1*^{6A} (Mohseni et al., 2009), UAS-*Atg1* RNAi (VDRC-16133), *Df (J4)* (Meng et al., 1999), UAS-*p35* (Hay et al., 1994), *Atg13*^{74} (Chang and Neufeld, 2009), *Atg18a*^{KG03090} (BL-13945), Df(3L)Exel6112 (BL-7591). The susceptibility of all Imd pathway mutants to pathogen infection was verified.

METHOD DETAILS

Axenic Fly Preparation: The fly embryos were collected on grape juice agar plates and later washed sequentially with 2.7% sodium hypochlorite solution, 70% Ethanol, sterile PBS and transferred to vials containing autoclaved fly food with an antibiotic cocktail of tetracycline, ampicillin, rifamycin (50 mg/ml, 500 mg/ml, or 200 mg/ml respectively). 16S ribosomal DNA PCR was performed to determine the axenic status of the flies, and whole fly lysates, from 10 animals, were serially diluted and plated on LB agar plates to quantify culturable microbes.

Immunostaining and Microscopy: Salivary glands were dissected in cold PBS solution and then fixed in 4% paraformaldehyde for overnight at 4°C. The glands were washed with PBST (PBS with 0.1% tween-20) and then with PBSBT (PBS with 0.1% tween-20 and 1% BSA). Next, they were incubated in PBSBT at room temperature for 2 hr and kept in primary antibody (rabbit anti-cleaved caspase-3, 1:400, Cell-Signaling, #9664) overnight at 4°C. The glands were washed with PBSBT, incubated with secondary antibody for 2 hr at room temperature and washed again with PBSBT for 1 hr. Finally, the glands were mounted in Vectashield (Vector Laboratories). For mCherry-Atg8 analysis, salivary glands were dissected in cold PBS and fixed with 2% paraformaldehyde for 1 hr in room temperature. The glands were then mounted in 50% glycerol containing 2 μM Hoechst stain. Imaging was

performed using Zeiss AxioImager microscope and mCherry-Atg8 puncta analysis and cell size measurement were performed with ImageJ software.

Quantitative RT-PCR analysis: Salivary glands were dissected in cold PBS and RNA isolated as described (Andres and Thummel, 1994). 500ng of total RNA was treated with DNaseI (Invitrogen) and used as template in an iScript cDNA synthesis reaction (Bio-Rad), followed by qPCR reaction using SYBR green supermix (Bio-Rad).

Histology: *Drosophila* flies were kept at 25°C and individual prepupa were also maintained at same temperature either for 6 or 24 hr. For histology experiments animals were fixed with FAAG solution (80% ethyl alcohol, 5% acetic acid, 1% glutaraldehyde, 4% Formaldehyde) overnight at 4C. Later fixed samples were paraffin embedded, sectioned with a microtome and stained with Weigert's Hematoxylin and Pollack Trichrome stains. Stained samples were visualized under a Zeiss Axiophot II microscope.

Induction of cell clones: To induce misexpression in clones of cells, virgin females of *yw hsFlp; pmCherry-Atg8a; Act > CD2 > GAL4, UAS-nlsGFP/TM6B* were crossed to indicated transgenic lines. An overnight egg lay was obtained at 25°C, and following the egg lay, embryos were heat shocked at 37°C for 15min.

Chromatin-Immunoprecipitation Assay: 4 different putative NFκB sites (−1706, −1229, −723, −23) upstream of the *Atg1* transcription start site were observed with the bioinformatic tools JASPER, Consite and MEME motif search. Another non-NFκB site (9284bp) inside the *Atg1* was chosen to rule out the possibility of non-specific binding of RelN to the *Atg1* locus.

Furthermore, *Diptericin* promoter region was used as a positive control as it has well-defined κB-sites (Meister et al., 1994), while the *Diedel* promoter was used as a negative control because this gene was completely unresponsive to RelishN expression in the salivary glands.

Wandering larvae were kept at 29°C for 3 hr to induce *Relish N-terminal* expression and ~100 pairs of salivary glands were dissected from these larvae. The glands were washed with cold PBS and then suspended in 1ml of PBS solution. The glands were cross-linked using 1% formaldehyde; at room temperature for 10 min. Glycine was added to quench the cross-linking at a concentration of 125mM. Then, the glands were washed with ice-cold TBS and resuspended with 500 mL of sonication buffer (50mM HEPES-pH7.8, 150mM NaCl, 1mM EDTA, 1% Triton X-100, 0.1% sodium deoxycholate, 1% SDS, Protease Inhibitor Cocktail). The glands were ground with pestle and then freeze-thawed. Finally, the solution was sonicated using the diagenode-bioruptor sonicator (20min sonication, 30sec On and 30sec Off cycle, setting-high). The chromatin was co-immunoprecipitated overnight using Dynabeads (Thermofisher, catalog no-10003D) conjugated with anti-FLAG antibody (Sigma, catalog no-F1804), reverse-crosslinked and purified. Quantitative RT-PCR was performed using primers designed to sites of interest.

QUANTIFICATION AND STATISTICAL ANALYSIS

Statistical analysis for all the numerical data was performed using GraphPad Prism 7.0a software. All figure legends include detailed information, for each panel, regarding the statistical tests applied as well as the exact number and type of samples. Variance is plotted as SEM throughout along with mean. No samples were excluded in these studies. Statistical significance required $p < 0.05$. Salivary gland histology was quantified by blindly scoring ~20 7 micron thick sections across each pupae, and a defect in salivary gland degradation required the observation of at least 2 sections with cell or gland fragments.

Supplementary Material

Refer to Web version on PubMed Central for supplementary material.

ACKNOWLEDGMENTS

We thank Bruno Lemaitre, Patrick Dolph, the BDSC, and VDRC for fly strains; and Tina Fortier and Alya Raphael for technical assistance. This work was supported by NIH grants RO1 AI099708 to N.S. and E.B. and AI060025 to N.S.

REFERENCES

Andres AJ, and Thummel CS (1994). Methods for quantitative analysis of transcription in larvae and prepupae. Methods Cell Biol 44, 565–573. [PubMed: 7535884]

Berry DL, and Baehrecke EH (2007). Growth arrest and autophagy are required for salivary gland cell degradation in Drosophila. Cell 131, 1137–1148. [PubMed: 18083103]

Bonizzi G, and Karin M (2004). The two NF-kappaB activation pathways and their role in innate and adaptive immunity. Trends Immunol 25, 280–288. [PubMed: 15145317]

Buchon N, Silverman N, and Cherry S (2014). Immunity in Drosophila melanogaster–from microbial recognition to whole-organism physiology. Nat. Rev. Immunol 14, 796–810. [PubMed: 25421701]

Cadwell K (2016). Crosstalk between autophagy and inflammatory signalling pathways: balancing defence and homeostasis. Nat. Rev. Immunol 16, 661–675. [PubMed: 27694913]

Cao Y, Chtarbanova S, Petersen AJ, and Ganetzky B (2013). Dnr1 muta-tions cause neurodegeneration in Drosophila by activating the innate immune response in the brain. Proc. Natl. Acad. Sci. USA 110, E1752–E1760. [PubMed: 23613578]

Chang YY, and Neufeld TP (2009). An Atg1/Atg13 complex with multiple roles in TOR-mediated autophagy regulation. Mol. Biol. Cell 20, 2004–2014. [PubMed: 19225150]

Chang TK, Shravage BV, Hayes SD, Powers CM, Simin RT, Wade Harper J, and Baehrecke EH (2013). Uba1 functions in Atg7- and Atg3-independent autophagy. Nat. Cell Biol 15, 1067–1078. [PubMed: 23873149]

Chinchore Y, Gerber GF, and Dolph PJ (2012). Alternative pathway of cell death in Drosophila mediated by NF-κB transcription factor Relish. Proc. Natl. Acad. Sci. USA 109, E605–E612. [PubMed: 22328149]

Choe KM, Werner T, Sto¨ven S, Hultmark D, and Anderson KV (2002). Requirement for a peptidoglycan recognition protein (PGRP) in Relish activation and antibacterial immune responses in Drosophila. Science 296, 359–362. [PubMed: 11872802]

Denton D, Chang TK, Nicolson S, Shravage B, Simin R, Baehrecke EH, and Kumar S (2012). Relationship between growth arrest and autophagy in midgut programmed cell death in Drosophila. Cell Death Differ 19, 1299–1307. [PubMed: 22555456]

DiAngelo JR, Bland ML, Bambina S, Cherry S, and Birnbaum MJ (2009). The immune response attenuates growth and nutrient storage in Drosophila by reducing insulin signaling. Proc. Natl. Acad. Sci. USA 106, 20853–20858. [PubMed: 19861550]

Fan Y, and Bergmann A (2010). The cleaved-Caspase-3 antibody is a marker of Caspase-9-like DRONC activity in Drosophila. Cell Death Differ 17, 534–539. [PubMed: 19960024]

Georgel P, Naitza S, Kappler C, Ferrandon D, Zachary D, Swimmer C, Kopczynski C, Duyk G, Reichhart JM, and Hoffmann JA (2001). Drosophila immune deficiency (IMD) is a death domain protein that activates antibacterial defense and can promote apoptosis. Dev. Cell 1, 503–514. [PubMed: 11703941]

Gottar M, Gobert V, Michel T, Belvin M, Duyk G, Hoffmann JA, Ferran-don D, and Royet J (2002). The Drosophila immune response against Gram-negative bacteria is mediated by a peptidoglycan recognition protein. Nature 416, 640–644. [PubMed: 11912488]

Guttridge DC, Albanese C, Reuther JY, Pestell RG, and Baldwin AS, Jr. (1999). NF-kappaB controls cell growth and differentiation through transcriptional regulation of cyclin D1. Mol. Cell. Biol 19, 5785–5799. [PubMed: 10409765]

Hay BA, Wolff T, and Rubin GM (1994). Expression of baculovirus P35 prevents cell death in Drosophila. Development 120, 2121–2129. [PubMed: 7925015]

Hayden MS, and Ghosh S (2011). NF-κB in immunobiology. Cell Res 21, 223–244. [PubMed: 21243012]

He C, and Klionsky DJ (2009). Regulation mechanisms and signaling pathways of autophagy. Annu. Rev. Genet 43, 67–93. [PubMed: 19653858]

Hedengren M, Asling B, Dushay MS, Ando I, Ekengren S, Wihlborg M, and Hultmark D (1999). Relish, a central factor in the control of humoral but not cellular immunity in Drosophila. Mol. Cell 4, 827–837. [PubMed: 10619029]

Imler JL, and Bulet P (2005). Antimicrobial peptides in Drosophila: structures, activities and gene regulation. Chem. Immunol. Allergy 86, 1–21. [PubMed: 15976485]

Kaneko T, Goldman WE, Mellroth P, Steiner H, Fukase K, Kusumoto S, Harley W, Fox A, Golenbock D, and Silverman N (2004). Monomeric and polymeric gram-negative peptidoglycan but not purified LPS stimulate the Drosophila IMD pathway. Immunity 20, 637–649. [PubMed: 15142531]

Kaneko T, Yano T, Aggarwal K, Lim JH, Ueda K, Oshima Y, Peach C, Erturk-Hasdemir D, Goldman WE, Oh BH, et al. (2006). PGRP-LC and PGRP-LE have essential yet distinct functions in the Drosophila immune response to monomeric DAP-type peptidoglycan. Nat. Immunol 7, 715–723. [PubMed: 16767093]

Karantza-Wadsworth V, Patel S, Kravchuk O, Chen G, Mathew R, Jin S, and White E (2007). Autophagy mitigates metabolic stress and genome damage in mammary tumorigenesis. Genes Dev 21, 1621–1635. [PubMed: 17606641]

Lee CY, Clough EA, Yellon P, Teslovich TM, Stephan DA, and Baehrecke EH (2003). Genome-wide analyses of steroid- and radiation-triggered programmed cell death in Drosophila. Curr. Biol 13, 350–357. [PubMed: 12593803]

Leulier F, Rodriguez A, Khush RS, Abrams JM, and Lemaitre B (2000). The Drosophila caspase Dredd is required to resist gram-negative bacterial infection. EMBO Rep 1, 353–358. [PubMed: 11269502]

Leulier F, Vidal S, Saigo K, Ueda R, and Lemaitre B (2002). Inducible expression of double-stranded RNA reveals a role for dFADD in the regulation of the antibacterial response in Drosophila adults. Curr. Biol 12, 996–1000. [PubMed: 12123572]

Leulier F, Parquet C, Pili-Floury S, Ryu JH, Caroff M, Lee WJ, Mengin-Lecreulx D, and Lemaitre B (2003). The Drosophila immune system detects bacteria through specific peptidoglycan recognition. Nat. Immunol 4, 478–484. [PubMed: 12692550]

Leulier F, Lhocine N, Lemaitre B, and Meier P (2006). The Drosophila inhibitor of apoptosis protein DIAP2 functions in innate immunity and is essential to resist gram-negative bacterial infection. Mol. Cell. Biol 26, 7821–7831. [PubMed: 16894030]

Li Q, and Verma IM (2002). NF-kappaB regulation in the immune system. Nat. Rev. Immunol 2, 725–734. [PubMed: 12360211]

Lin L, Rodrigues F, Kary C, Contet A, Logan M, Baxter RHG, Wood W, and Baehrecke EH (2017). Complement-related regulates autophagy in neighboring cells. Cell 170, 158–171.e8. [PubMed: 28666117]

Mathew R, Kongara S, Beaudoin B, Karp CM, Bray K, Degenhardt K, Chen G, Jin S, and White E (2007). Autophagy suppresses tumor progression by limiting chromosomal instability. Genes Dev 21, 1367–1381. [PubMed: 17510285]

Meister M, Braun A, Kappler C, Reichhart JM, and Hoffmann JA (1994). Insect immunity. A transgenic analysis in Drosophila defines several functional domains in the diptericin promoter. EMBO J 13, 5958–5966. [PubMed: 7813433]

Meng X, Khanuja BS, and Ip YT (1999). Toll receptor-mediated Drosophila immune response requires Dif, an NF-kappaB factor. Genes Dev 13, 792–797. [PubMed: 10197979]

Meyer SN, Amoyel M, Bergantin˜os C, de la Cova C, Schertel C, Basler K, and Johnston LA (2014). An ancient defense system eliminates unfit cells from developing tissues during cell competition. Science 346, 1258236. [PubMed: 25477468]

Mizushima N, and Komatsu M (2011). Autophagy: renovation of cells and tissues. Cell 147, 728–741. [PubMed: 22078875]

Mohseni N, McMillan SC, Chaudhary R, Mok J, and Reed BH (2009). Autophagy promotes caspase-dependent cell death during Drosophila development. Autophagy 5, 329–338. [PubMed: 19066463]

Pengo N, Scolari M, Oliva L, Milan E, Mainoldi F, Raimondi A, Fagioli C, Merlini A, Mariani E, Pasqualetto E, et al. (2013). Plasma cells require autophagy for sustainable immunoglobulin production. Nat. Immunol 14, 298–305. [PubMed: 23354484]

Petersen AJ, Katzenberger RJ, and Wassarman DA (2013). The innate immune response transcription factor relish is necessary for neurodegeneration in a Drosophila model of ataxia-telangiectasia. Genetics 194, 133–142. [PubMed: 23502677]

Pham LN, Dionne MS, Shirasu-Hiza M, and Schneider DS (2007). A specific primed immune response in Drosophila is dependent on phagocytes. PLoS Pathog 3, e26. [PubMed: 17352533]

Qin ZH, Wang Y, Kegel KB, Kazantsev A, Apostol BL, Thompson LM, Yoder J, Aronin N, and DiFiglia M (2003). Autophagy regulates the processing of amino terminal huntingtin fragments. Hum. Mol. Genet 12, 3231–3244. [PubMed: 14570716]

Qu X, Yu J, Bhagat G, Furuya N, Hibshoosh H, Troxel A, Rosen J, Eskelinen EL, Mizushima N, Ohsumi Y, et al. (2003). Promotion of tumorigenesis by heterozygous disruption of the beclin 1 autophagy gene. J. Clin. Invest 112, 1809–1820. [PubMed: 14638851]

Rus F, Flatt T, Tong M, Aggarwal K, Okuda K, Kleino A, Yates E, Tatar M, and Silverman N (2013). Ecdysone triggered PGRP-LC expression controls Drosophila innate immunity. EMBO J 32, 1626–1638. [PubMed: 23652443]

Saitoh T, Fujita N, Jang MH, Uematsu S, Yang BG, Satoh T, Omori H, Noda T, Yamamoto N, Komatsu M, et al. (2008). Loss of the autophagy protein Atg16L1 enhances endotoxin-induced IL-1beta production. Nature 456, 264–268. [PubMed: 18849965]

Schmid D, Pypaert M, and Münz C (2007). Antigen-loading compartments for major histocompatibility complex class II molecules continuously receive input from autophagosomes. Immunity 26, 79–92. [PubMed: 17182262]

Scott RC, Juha´sz G, and Neufeld TP (2007). Direct induction of autophagy by Atg1 inhibits cell growth and induces apoptotic cell death. Curr. Biol 17, 1–11. [PubMed: 17208179]

Takehana A, Yano T, Mita S, Kotani A, Oshima Y, and Kurata S (2004). Peptidoglycan recognition protein (PGRP)-LE and PGRP-LC act synergistically in Drosophila immunity. EMBO J 23, 4690–4700. [PubMed: 15538387]

Thorburn A, Thamm DH, and Gustafson DL (2014). Autophagy and cancer therapy. Mol. Pharmacol 85, 830–838. [PubMed: 24574520]

Vidal S, Khush RS, Leulier F, Tzou P, Nakamura M, and Lemaitre B (2001). Mutations in the Drosophila dTAK1 gene reveal a conserved function for MAPKKKs in the control of rel/NF-kappaB-dependent innate immune responses. Genes Dev 15, 1900–1912. [PubMed: 11485985]

White E (2015). The role for autophagy in cancer. J. Clin. Invest 125, 42–46. [PubMed: 25654549]

Wiklund ML, Steinert S, Junell A, Hultmark D, and Sto¨ven S (2009). The N-terminal half of the Drosophila Rel/NF-kappaB factor Relish, REL-68, constitutively activates transcription of specific Relish target genes. Dev. Comp. Immunol 33, 690–696. [PubMed: 19135474]

Yano T, Mita S, Ohmori H, Oshima Y, Fujimoto Y, Ueda R, Takada H, Goldman WE, Fukase K, Silverman N, et al. (2008). Autophagic control of listeria through intracellular innate immune recognition in Drosophila. Nat. Immunol 9, 908–916. [PubMed: 18604211]

Yu WH, Kumar A, Peterhoff C, Shapiro Kulnane L, Uchiyama Y, Lamb BT, Cuervo AM, and Nixon RA (2004). Autophagic vacuoles are enriched in amyloid precursor protein-secretase activities: implications for betaamyloid peptide over-production and localization in Alzheimer's disease. Int. J. Biochem. Cell Biol 36, 2531–2540. [PubMed: 15325590]

Highlights

- NF-κB family member *Relish* and PGRPs are required for salivary gland degradation
- Canonical NF-κB signaling and microflora are not involved in this pathway
- *Relish* influences autophagy, but not caspases, during cell death
- The *Atg1* autophagy gene is transcriptionally regulated by *Relish*

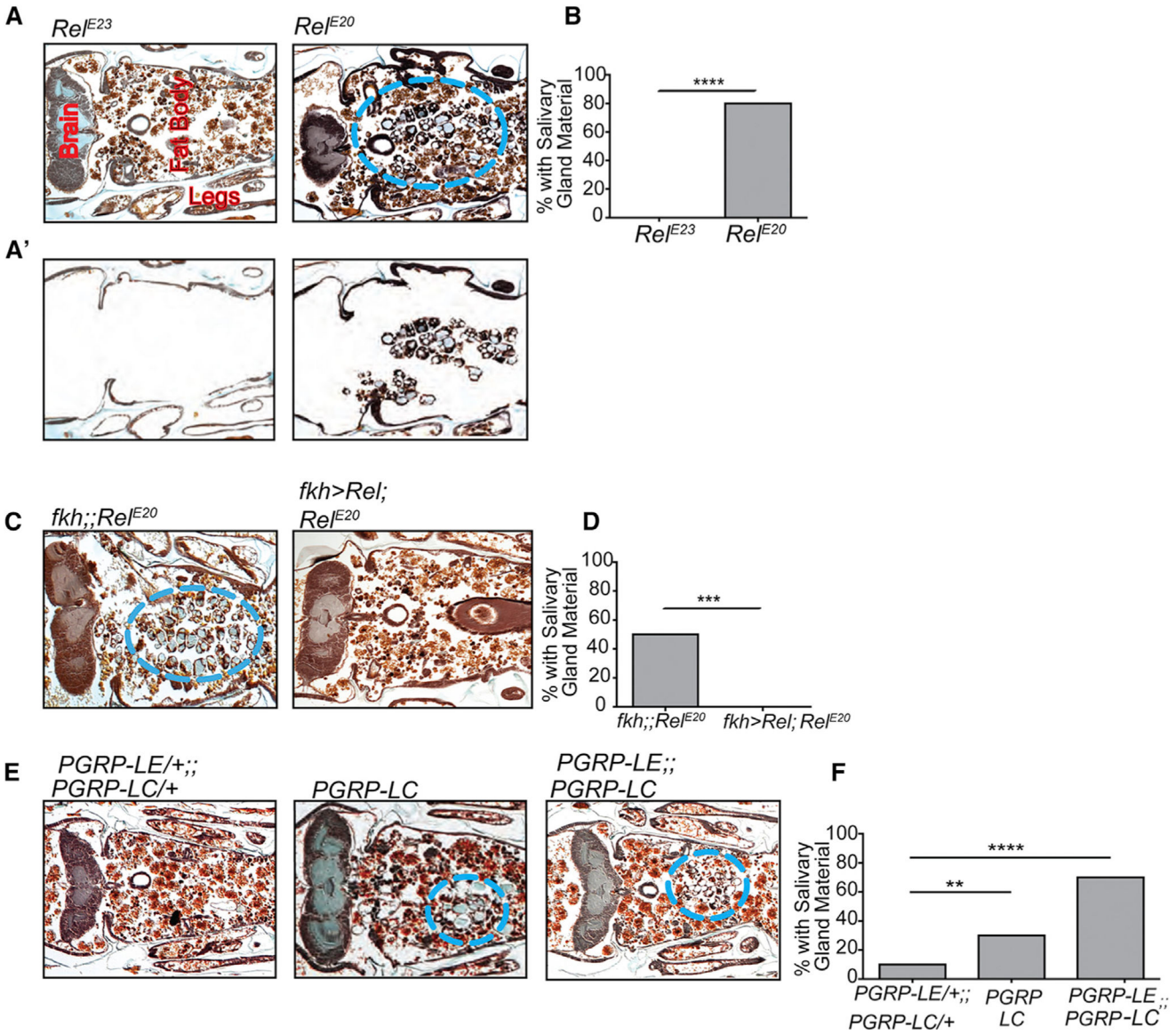

Figure 1. The *Drosophila* NF-κB Factor Relish Is Essential for Salivary Gland Degradation

(A) Representative histological sections of control (*Rel* ^{E23}) and *Relish* mutant (*Rel*^{E20}) flies 24 hr APF. Anatomical features are noted in the left panel, and salivary gland fragments observed in the *Relish* mutants are highlighted within dotted blue circle.

(A‘) Representative histological sections of control (*Rel*^{E23}, left) and Relish mutant (*Rel*^{E20}, right) 24 hr APF. All tissues except the salivary gland cellular fragments were removed in Photoshop.

(B) Quantitation of histology from 20 independent pupae for each strain as in (A). Statistical analysis by chi-square test.

(C) Representative histological sections of samples of control *Relish* mutants (*fkh-Gal4*/+;; *Rel*^{E20}, left), and *Relish* mutants with salivary-gland-specific expression of transgenic *Relish* (*fkh-Gal4*/+; *UAS-Relish/+*; *Rel*^{E20}, right) analyzed 24 hr APF. Salivary gland fragments are highlighted within dotted blue circle.

(D) Quantitation of histology from 20 independent pupae for each strain as in (C). Statistical analysis by chi-square test.

(E) Representative histological sections of control (*PGRP-LE*^{112}/+;; *PGRP-LCx*$^{\Delta E}$ /+, left) and *PGRP-LC* mutants (*PGRP-LCx*$^{\Delta E}$, middle) and *PGRP-LC* and *PGRP-LE* double mutants (*PGRP-LE*^{112};; *PGRP-LCx*$^{\Delta E}$, right) flies 24 hr APF. Salivary gland fragments observed in *PGRP* mutants are highlighted within dotted blue circle.

(F) Quantitation of histology from 20 independent pupae for each strain as in (E). Statistical analysis by chi-square test.

****p < 0.0001, ***p < 0.001, **p < 0.01. See also Figures S1, S2, S3, and S4.

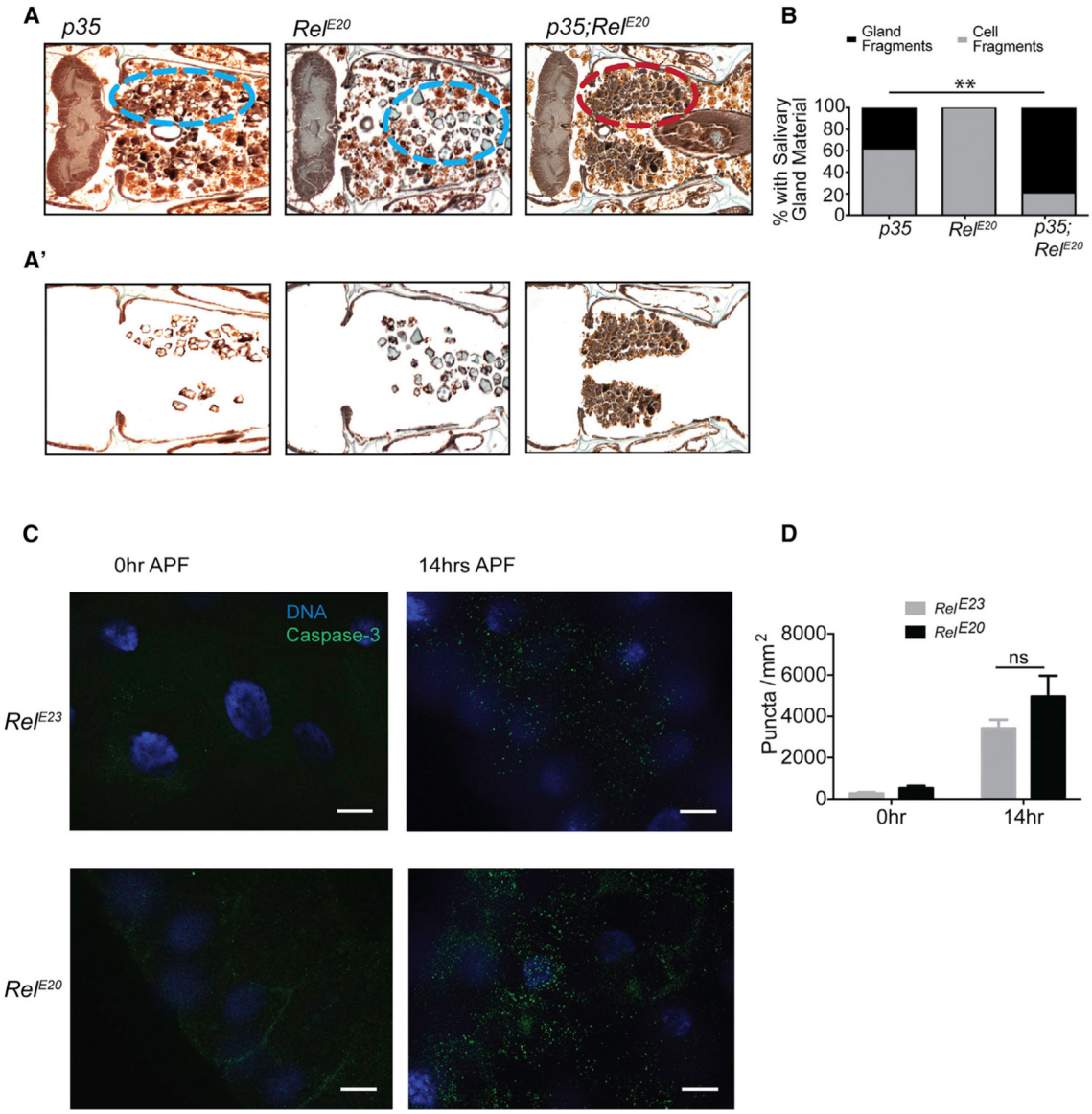

Figure 2. Relish Controls Salivary Gland Degradation Independent of Caspase Activity

(A) epresentative histological sections of animals with salivary-gland-specific expression of *p35* (*fkh-gal4/+;* UAS-*p35/+; Rel*^{E20}*/+*, left), *Relish* mutants (UAS-*p35; Rel*^{E20}, middle), and *Relish* mutants with salivary-gland-specific expression of *p35* (*fkh-gal4/+;* UAS-*p35/+; Rel*^{E20}, right) 24 hr APF. Salivary gland cell fragments are within dotted blue, and gland fragments are within dotted red circle.

(A‘) Representative histological sections of animals with salivary-gland-specific expression of *p35* (*fkh-gal4/+;* UAS-*p35/+; Rel*^{E20}*/+*, left), *Relish* mutants (UAS-*p35; Rel*^{E20}, middle), and *Relish* mutants with salivary-gland-specific expression of *p35* (*fkh-gal4/+;* UAS-*p35/+; Rel*^{E20}, right) 24 hr APF. All tissues except the salivary gland cellular fragments and gland fragments were removed in Photoshop.

(B) Quantitation of histology from 21, 23, and 24 independent pupae, respectively, for each strain as in (A). Statistical analysis by chi-square test comparing gland fragments in the *p35* only versus *p35*, *Relish* strains. **p < 0.01.

(C) Cleaved caspase-3 antibody staining (green) and DAPI (blue) in salivary glands of control (Rel^{E23}) and mutant (Rel^{E20}) animals at 0 hr and 14 hr APF. Scale bar, 25 μm.

(D) Quantitation of cleaved caspase-3 puncta in salivary glands of control (Rel^{E23}) and mutant (Rel^{E20}) animals at 0 hr and 14 hr APF (n = 7 salivary glands). Data presented as mean ± SEM, and statistical analysis by unpaired two-tailed t test with Welch's correction. ns, not significant.

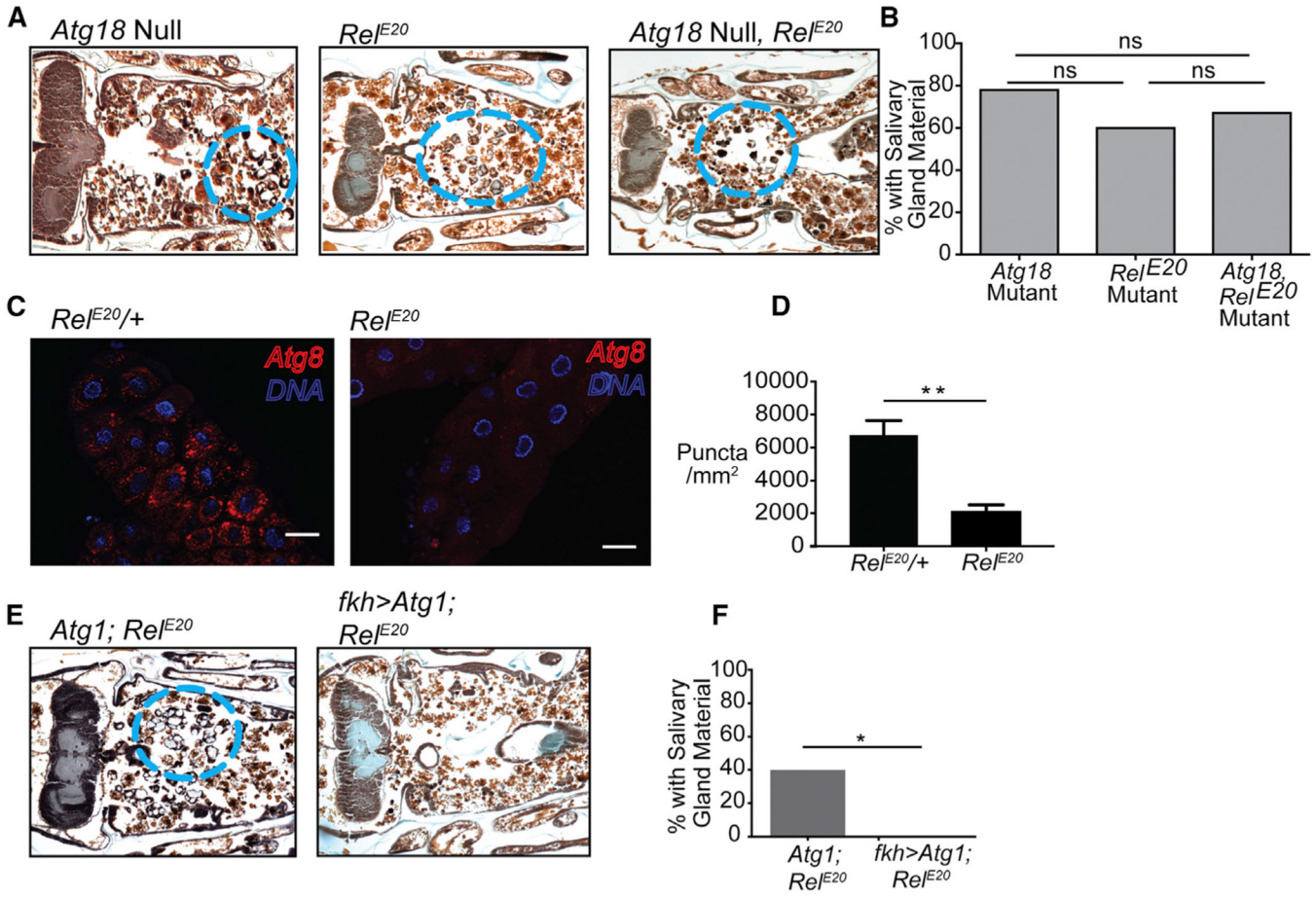

Figure 3. *Relish*-Mediated Salivary Gland Degradation Is Autophagy Dependent

(A) Representative histological sections 24 hr APF of *Atg18* mutants (left, $Atg18^{KG03090}$/Df(3L)^{Exel6112}); *Relish* mutant (middle, $Atg18^{KG03090}$, Rel^{E20}/Rel^{E20}); and *Atg18*, *Relish* double mutants (right, if/CyO; $Atg18^{KG03090}$, Rel^{E20}/Df(3L)^{Exel6112}, Rel^{E20}). Salivary gland fragments are within blue dotted circle.

(B) Quantitation of histology from 9, 10, and 12 independent pupae for each genotype as in (A), respectively. Statistical significance by chi-square test. ns, not significant.

(C) Representative images of mCherry-Atg8a expressed in the salivary glands of control animals (w; *pmCherry-Atg8a*; Rel^{E20}/TM6b) or *Relish* null mutants (w; *pmCherry-Atg8a*; Rel^{E20}). Salivary glands were dissected and visualized 14 hr APF. Image scale bar, 50 μm.

(D) Quantitation of mCherryAtg8a-puncta from 5 independent salivary glands for each genotype as in (C). Data presented as mean ± SEM, and statistical analysis by unpaired two-tailed t test with Welch's correction. **$p < 0.01$.

(E) Representative histological sections of *Relish* mutants (UAS-$Atg1^{6A}$; Rel^{E20}, left), and *Relish* mutants with transgenic salivary-gland-specific *Atg1* expression, (*fkh-Gal4*/+; UAS-$Atg1^{6A}$ /+; Rel^{E20}, right) analyzed 24 hr APF. Salivary gland fragments are highlighted within dotted blue circle.

(F) Quantitation of histology from 20 independent pupae for each strain as in (E). Statistical analysis by chi-square test. *$p < 0.05$.

See also Figure S4.

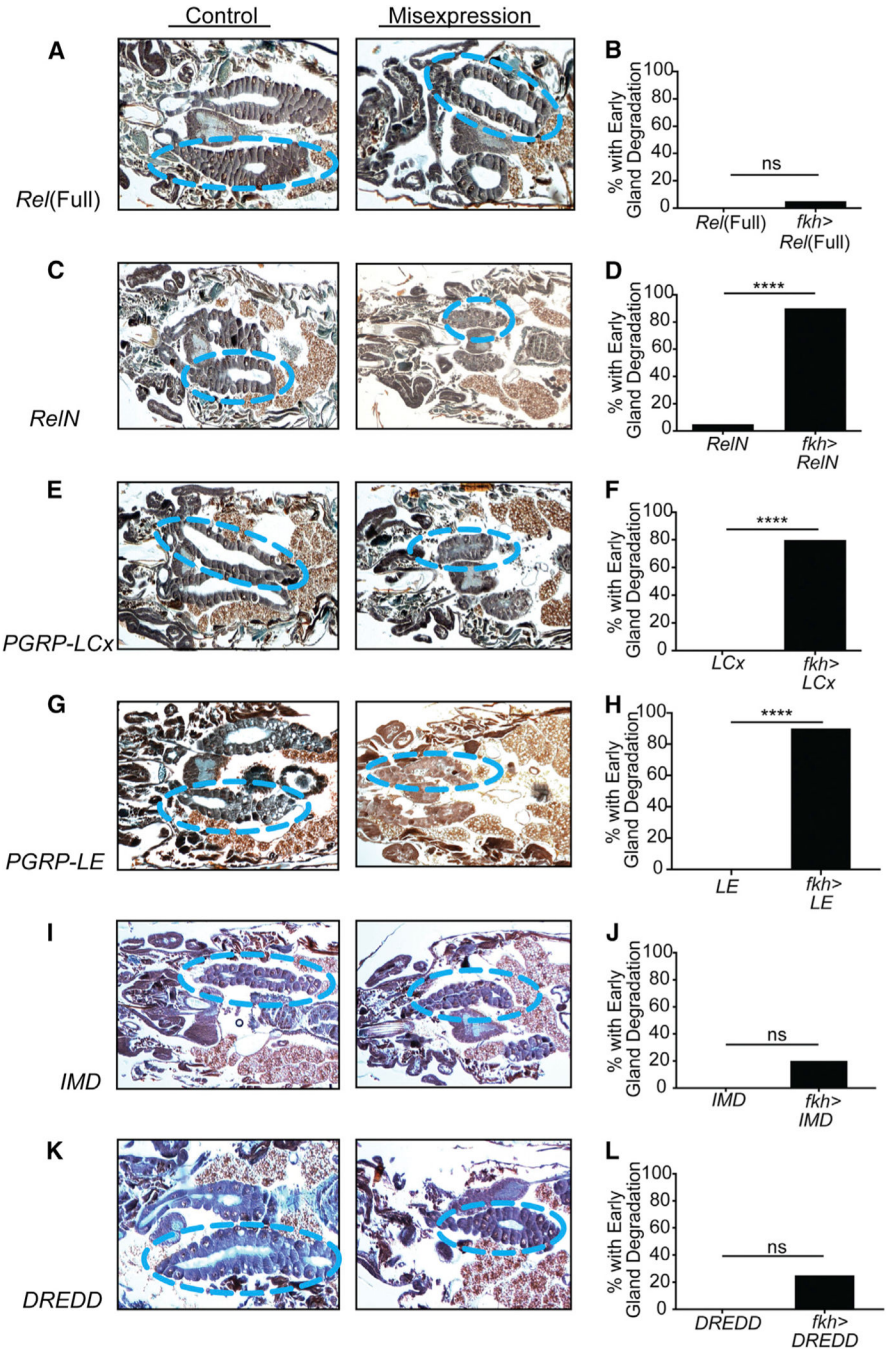

Figure 4. *Relish-N* or *PGRP-LC* Misexpression Causes Premature Gland Degradation

(A and B) Representative histological sections from 6 hr APF of control animals (left, w; UAS-*Relish* full-length,) and animals expressing *Relish* full-length ectopically in salivary glands (right, w; UAS-*Relish* full-length /+; *fkh-Gal4*/+) (A). Salivary glands are highlighted within blue dotted circles. (B) Quantitation of histological sections from 20 independent pupae as in (A). Statistical significance by chi-square test. ns not significant.

(C and D) Representative histological sections from 6 hr APF of control animals (left, UAS-*RelN*, w) and animals expressing *Relish N-terminal* ectopically in salivary glands (right,

UAS-*RelN*/+;; *fkh-Gal4*/+) (C). Salivary glands are highlighted within blue dotted circles. (D) Quantitation of histological sections from 20 independent pupae as in (C). Statistical significance by chi-square test. ****p < 0.0001.

(E and F) Representative histological sections from 6 hr APF of control animals (left, w; UAS-*PGRP-LCx*) and animals expressing *PGRP-LCx* ectopically in salivary glands (right, w; UAS-*PGRP-LCx*/+; *fkh-Gal4*/+) (E). Salivary glands are highlighted within blue dotted circles. (F) Quantitation of histological sections from 20 independent pupae as in (E). Statistical significance by chi-square test. ****p < 0.0001.

(G and H) Representative histological sections from 6 hr APF of control animals (left, w; UAS-*PGRP-LE*) and animals expressing *PGRP-LE* ectopically in salivary glands (right, w;UAS-*PGRP-LE*/+; *fkh-Gal4*/+) (G) Salivary glands are highlighted within blue dotted circles. (H) Quantitation of histological sections from 20 independent pupae as in (G). Statistical significance by Chi-square test. ****p < 0.0001.

(I and J) Representative histological sections from hr APF of control animals (left, w; UAS-*imd*) and animals expressing *imd* ectopically in salivary glands (right, w;UAS-*imd*/+; *fkh-Gal4*/+) (I). Salivary glands are highlighted within blue dotted circles. (J) Quantitation of histological sections from 20 independent pupae as in (I). Statistical significance by chi-square test. ns, not significant.

(K and L) Representative histological sections from 6 hr APF of control animals (left, w;; UAS-*Dredd*) and animals expressing *Dredd* ectopically in salivary glands (right, w;;UAS-*Dredd*/*fkh-Gal4*) (K). Salivary glands are highlighted within blue dotted circles. (L) Quantitation of histological sections from 20 independent pupae as in (K). Statistical significance by chi-square test. ns, not significant. See also Figures S5 and S6.

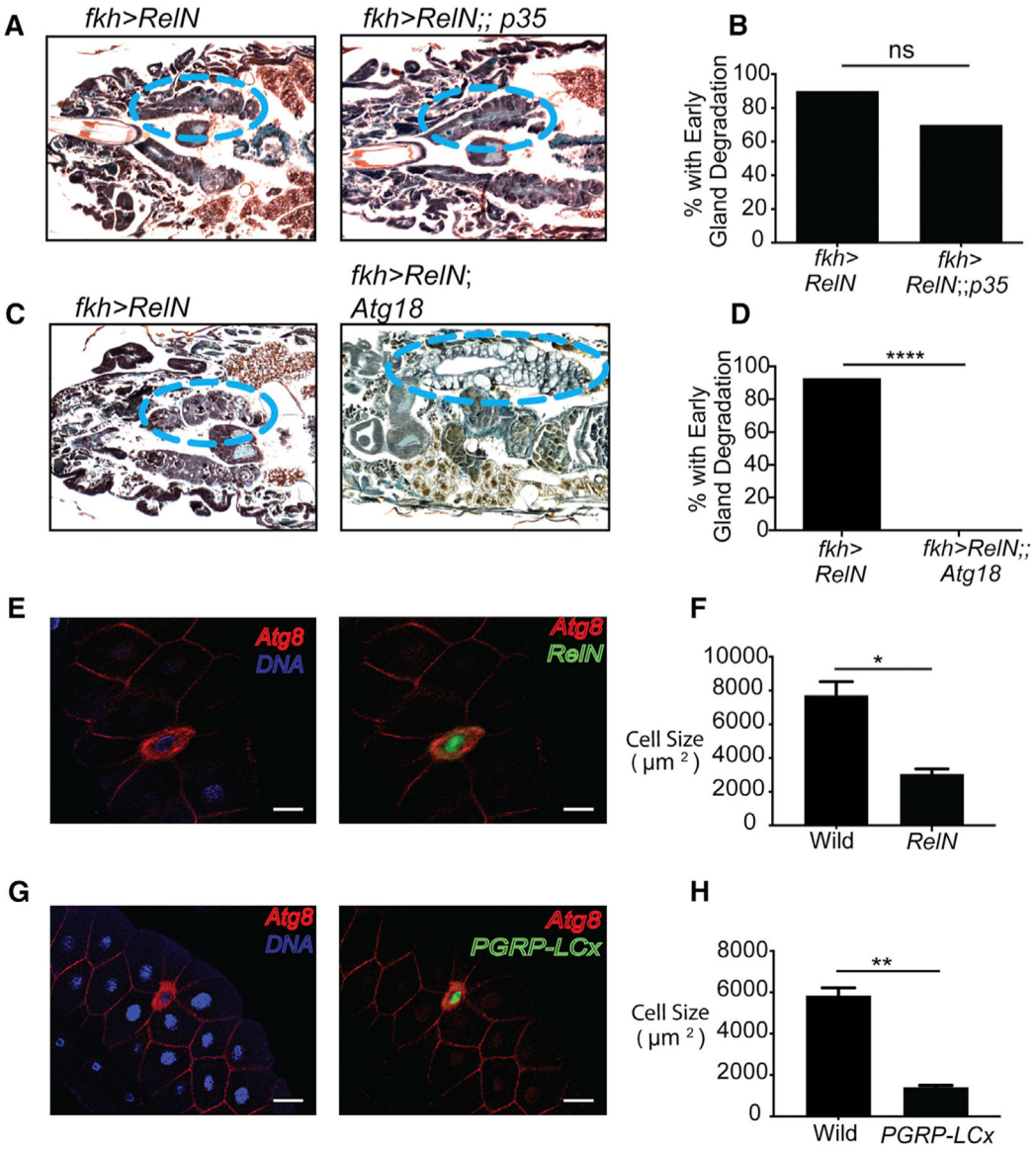

Figure 5. *Relish-N*- and *PGRP-LC*-Mediated Early Gland Degradation Is Autophagy Dependent

(A) Representative histological sections of animals expressing *RelN* (left, UAS-*RelN*/+;; *fkh-Gal4*/+) and animals expressing *RelN* and *p35* together (UAS-*RelN*/+;; *fkh-Gal4*/UAS-*p35*) in salivary glands 6 hr APF. Salivary glands are highlighted within blue dotted circles.

(B) Quantitation of histology from 20 pupae for each genotype as in (A). Statistical significance by chi-square test. ns, not significant.

(C) Representative histological sections of ani-mals expressing *RelN* in salivary glands of wild-type flies (left, UAS-*RelN*/+;; *fkh-Gal4*/+) and in *Atg18* mutant flies (right, UAS-*RelN*/*fkh-Gal4*;; $Atg18^{KG03090}$/*Df (3L) Exel6112*) 6 hr APF. Salivary glands are highlighted within blue dotted circles.

(D) Quantitation of 14 and 10 independent pupae, respectively, from each genotype as in (C). Statistical significance by chi-square test. ****$p < 0.0001$, ns not significant.

(E and F) Representative images of dissected salivary glands from wandering larvae (E). All cells express *mCherryAtg8*, while RelN is expressed in GFP marked clone cells (*hsflp/*UAS-*RelN; pmCherryAtg8/CyO*; *act < FRT*, *cd2*, *FRT > Gal4*; UAS-*GFP*/+). Quantitation of the cell size of RelN expressing cells compared to neighboring wild-type cells is shown in (F). n = 3 salivary glands. Data presented as mean ± SEM, and statistical analysis by unpaired two-tailed t test with Welch's correction. *$p < 0.05$.

(G and H) Representative images of dissected salivary glands from wandering larvae (G). All cells express *mCherryAtg8*, while *PGRP-LCx* is expressed in GFP marked clone cells (*hsflp/w*; *pmCherryAtg8/*UAS-*PGRP-LCx*; *act < FRT*, *cd2*, *FRT > Gal4*; UAS-*GFP*/+). Scale bar, 25 μm. Quantitation of the cell size of *PGRP-LCx* expressing cells and wild-type cells is shown in (H). n = 3 salivary glands. Data presented as mean ± SEM, and statistical analysis by unpaired two-tailed t test with Welch's correction. **$p < 0.01$.

See also Figure S6.

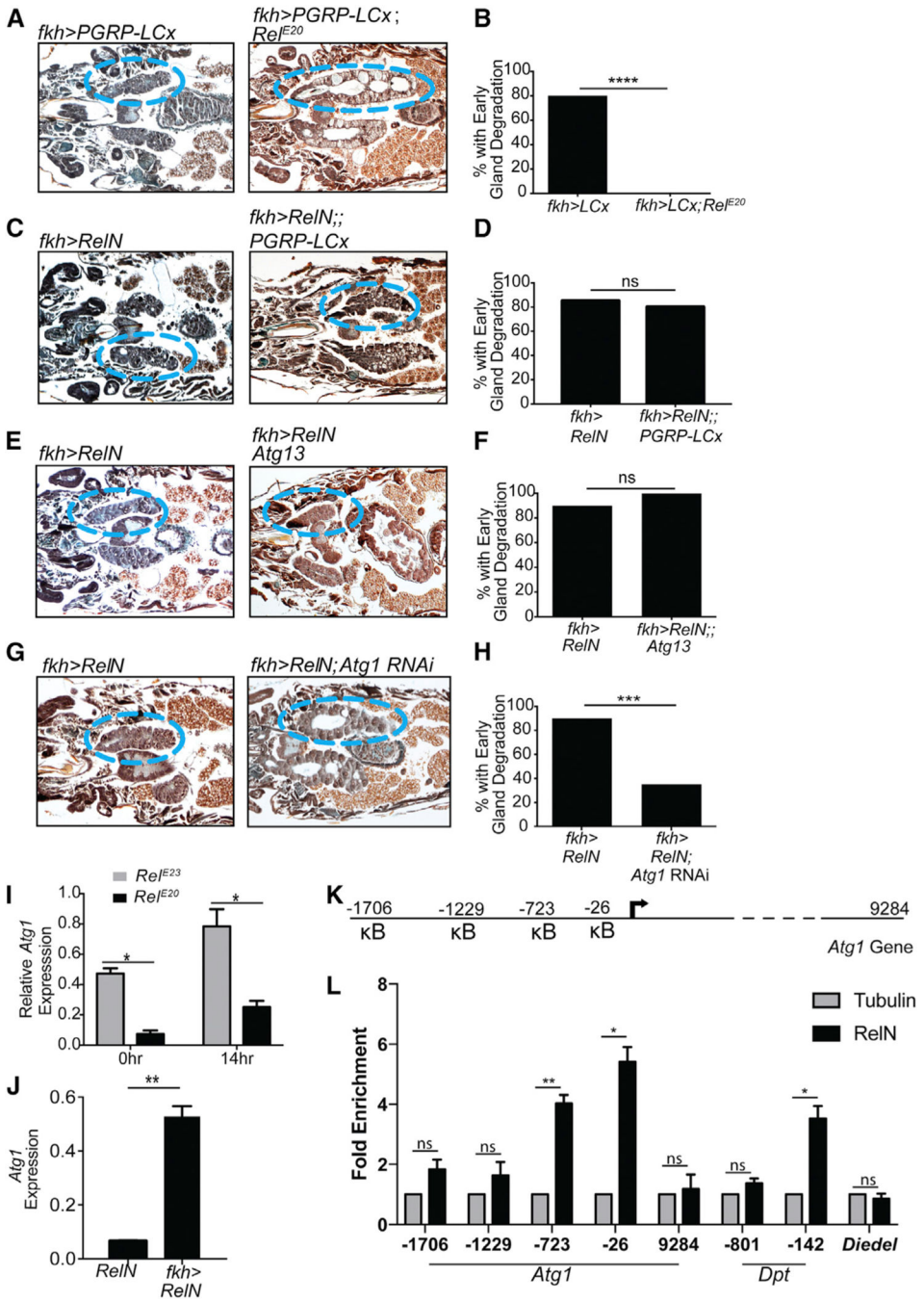

Figure 6. *Relish* Controls Autophagy through *Atg1* Expression

(A) Representative histological sections of animals expressing *PGRP-LCx* in salivary glands of wild-type flies (left, w; UAS-*PGRP-LCx*/+; *fkh-Gal4*/+) and *Relish* mutant flies (right, *fkh-Gal4*/+; UAS-*PGRP-LCx*/+; Rel^{E20}) 6 hr APF.

(B) Quantitation of 20 independent pupae from each genotype as in (A). Statistical significance by chi-square test.

(C) Representative histological sections of animals expressing *RelN* in salivary glands of wild-type flies (left, UAS-*RelN*/+;; *fkh-Gal4*/+) and in *PGRP-LCx* mutant flies (right, UAS-*RelN*/*fkh-gal4*;; *PGRP-LCx*$^{\Delta E}$) 6 hr APF.

(D) Quantitation of 20 independent pupae, respectively, from each genotype as in (C). Statistical significance by chi-square test.

(E) Representative histological sections of animals expressing *RelN* in salivary glands of wild-type flies (left, UAS-*RelN*/+;; *fkh-Gal4*/+) and in *Atg13* mutant flies (right, UAS-*RelN*/+;; *fkh-gal4*, *Atg13*^{74}) 6 hr APF.

(F) Quantitation of 10 and 11 independent pupae, respectively, from each genotype as in (E). Statistical significance by chisquare test.

(G) Representative histological sections of animals expressing *RelN* (left, UAS-*RelN*/+;; *fkh-Gal4*/+) and animals expressing *RelN* and *Atg1* RNAi together (UAS-*RelN*/+; UAS-*Atg1* RNAi/+; *fkh-Gal4*/+) in salivary glands 6 hr APF.

(H) Quantitation of histology from 20 pupae for each genotype as in (G). Statistical significance by chi-square test. For (A), (C), and (E), salivary glands are highlighted within blue dotted circles.

(I) *Atg1* gene expression levels in salivary glands of control (*Rel*^{E23}) and *Rel*^{E20} animals at 0 hr and 14 hr APF, measured by qRT-PCR. n = 3 independent RNA samples, each collected from 30 salivary glands. Data presented as mean ± SEM, and statistical analysis by unpaired two-tailed t test with Welch's correction.

(J) *Atg1* gene expression in salivary glands of control (UAS-*RelN*) and *RelN* expressing animals (UAS-*RelN*/+;; *fkh-Gal4*/+) 6 hr APF, quantified by qRT-PCR. n = 3 independent RNA samples, each collected from 30 salivary glands. Data presented as mean ± SEM, and statistical analysis by unpaired two-tailed t test with Welch's correction.

(K) The putative NF-κB sites in the promoter region (1706 bp, 1229 bp, 723 bp, 26 bp) and transcription initiation site of the *Atg1* genes are indicated in the diagram, as well as the downstream region (9284), which was used as a negative control.

(L) Chromatin immunoprecipitation (ChIP) analysis of the recruitment of Relish-N to the promoters of *Diedel*, *Atg1*, and *Diptericin* in salivary glands. *Diedel* and *Diptericin* were used as negative and positive controls, respectively. All values are represented as fold enrichment. Glands from the RelN expressing strain (UAS-FLAG-*RelN*/+; tub-Gal80^{ts}/+; *fkh-Gal4*/+) were compared to the driver only control strain (w; tub-Gal80^{ts}; *fkh-Gal4*). n = 3 independent chromatin samples, each collected from 150 salivary glands.

****p < 0.0001, ***p < 0.001, **p < 0.01, *p < 0.05. ns, not significant. See also Figure S6.